Yi and Amelin
Journal of Analytical Science and Technology (2024) 15:27
https://doi.org/10.1186/s40543-024-00439-z

Journal of Analytical Science and Technology

RESEARCH ARTICLE Open Access

SIMS study of fine-scale distribution of U, Th and Pb in meteorites

Keewook Yi[1*] and Yuri Amelin[1]

Abstract

We report developing a procedure for measuring concentrations of U, Th and Pb (including all natural Pb isotopes) to establish the distribution of these elements in meteorite minerals and correctly interpret Pb-isotopic ages of meteorites. The concentrations were measured on KBSI SHRIMP IIe by peak jumping using a discrete-dynode secondary electron multiplier. The concentrations were calculated relative to BCR-2G glass and monitored by analysis of the NIST glasses SRM-615 and SRM-617 as secondary reference materials. The detection limits using the spot sizes of ca. 180 μm^2, primary O_2^- beam current of 10.6 nA, and with amplifier dark noise of 0.015 counts per second are ~ 0.2 parts per billion (ppb) for U (500 s integration), ~ 0.6 ppb for Pb (100 s integration for each of the major isotopes), and ~ 1.2 ppb for Th (100 s integration). Analyses of the NIST glasses confirm that the measured concentrations of U and Th are consistent with their certified values, while the Pb concentrations are about four times too low, most likely due to the compositional mismatch between the primary and secondary reference materials. The achieved level of sensitivity and concentration precision (~ 20–30%) is adequate for measuring U, Th and Pb distributions in both rock-forming and accessory minerals in chondrites, achondrites, and their components.

Keywords Geochronology, Isotopic dating, U-Pb, SIMS, Trace element concentrations, Uranium, Thorium, Meteorites, Cosmochemistry

Introduction

The dating method based on decay of ^{238}U and ^{235}U and accumulation of radiogenic ^{206}Pb and ^{207}Pb is widely used to study meteorite chronology. Unlike terrestrial and planetary igneous rocks, meteorites derived from asteroids rarely contain U-rich accessory minerals such as zircon or baddeleyite. In order to date the rocks originating from asteroids with the U–Pb method, we have to rely mainly on analysis of whole rocks and rock-forming minerals and apply sample treatments (e.g., acid leaching) that selectively remove non-radiogenic Pb, while leaving most U and radiogenic Pb in the solid. In order to accurately interpret Pb-isotopic dates calculated from these analyses, we need information about the minerals that contain U and radiogenic Pb: what these minerals are, what is their abundance, grain size, and Pb and U concentrations, whether they are primary or secondary, how fast is the rate of diffusion of Pb and U in these minerals, whether U and radiogenic Pb are located in the crystal lattice or in inclusions.

Bulk concentration of U in meteorites varies from below 10 ppb to ca. 300 ppb (Amelin 2015). The median U concentrations are between 8 and 26 ppb in ordinary, enstatite and carbonaceous chondrites, and 100–128 ppb in eucrites, angrites, and Ca-Al rich refractory inclusions (CAIs) in CV chondrites. The distribution of these elements between mineral phases is extremely uneven (e.g., Goreva and Burnett 2001, and references therein). Concentrations of U and Th in chondrites and achondrites can reach parts per million level in Ca-phosphates apatite and merrillite, and in rare minerals such as perovskite, but the concentrations of these elements in most

*Correspondence:
Keewook Yi
kyi@kbsi.re.kr
[1] Korea Basic Science Institute, 162 Yeongudanji-ro, Ochang, Cheongju, Chungbuk 28119, Republic of Korea

other minerals are below the bulk rock values. These low concentrations prevent measurements of U distribution in meteorites by the commonly used analytical with micron-scale spatial resolution, such as laser ablation ICPMS and synchrotron radiation XRF, let alone less sensitive methods such as electron microprobe. The two analytical methods that have been demonstrated to combine adequate sensitivity with high spatial resolution are fission track radiography and large ion microprobe (SIMS) analysis. Fission track radiography was first applied to meteorite research in the late 1970's and 1980's and was used in the pioneering studies of U and Th distribution in meteorite components (Jones and Burnett 1979; Crozaz 1979; Burnett et al. 1982). However, this method can be used only for determination of the elements that can undergo nuclear fission, i.e., U and Th. In contrast, high-sensitivity SIMS, such as SHRIMP or Cameca 1270–1300 series, allows including the isotopes of other elements, irrespective of their nuclear properties, in the analytical sequence, while reaching similar or higher sensitivity for U and Th than fission track radiography. This allows us to measure concentrations of all Pb isotopes along with U and Th—a major advantage if we consider application of element distributions to interpretation of the U–Pb age data.

In this study, we describe a recently developed procedure for measuring the distribution of U, Th and Pb in meteorites and their components using SHRIMP IIe at the Korea Basic Science Institute. This procedure was applied to analysis of angrites, eucrites, and Ca-Al-rich refractory inclusions (CAIs) from Allende CV chondrite. Here, we only discuss the procedure and its analytical performance. The distribution of U, Th and Pb in the studied materials and the discussion of its cosmochemical significance will be presented elsewhere.

Methods

The procedure for analysis of distribution of U, Th and Pb in meteorites described here is based on the previous similar developments at the Geological Survey of Canada (Amelin et al. 2003), Australian National University (Merle et al. 2020, Datta et al. 2023 submitted) and Swedish Museum of Natural History (Bollard et al. 2017).

Thin slabs of achondrites were mounted in 25-mm epoxy casts and prepared using the standard procedure adopted at KBSI for SIMS-based U–Pb zircon geochronology. The mounts were polished using diamond slurries with crystal sizes of 9, 3 and 1 μm, and additionally polished at KOPRI with the 0.3–0.5 μm diamond slurries to improve the smoothness of the surface, coated with a thin (~ 20 nm) layer of carbon, and imaged with a field emission electron probe microanalyser using WDS detectors to achieve adequate sensitivity. This imaging produced X-ray maps for Na, Si, Ca, Fe, Ti, Mg, Al, P, Mn and Cr, as well as BSE and SE images. The images with the size of 2570 to 3800 pixels on the long side, and between 1510 and 2710 pixels on the short side, have sufficiently high resolution for precise positioning of the primary ion beam in subsequent SIMS analyses.

The CAI mounts were provided by F. Tissot, California Institute of Technology. These mounts were previously imaged at the University of Hawaii, and some were analysed for ^{26}Al-^{26} Mg systematics using SIMS. When received at KBSI, these mounts already had carbon coating at the surface, so they were just cleaned from possible dust particles by blowing filtered air, and coated with an additional ~ 20 nm layer of carbon to assure adequate surface conductivity. Three out of four mounts were first analysed for oxygen isotope composition on the KBSI Cameca ims 1300 ion microprobe, and then for U, Th and Pb distribution on SHRIMP IIe using the procedure described below.

The U, Th, Pb distribution analyses on KBSI SHRIMP are run in two sessions. During the first session (analyses of two angrites and an eucrite in July–August 2023), the samples were analysed using primary O_2^- ion beam with intensity of 7.5 ± 0.5 (SD) nA, focussed to an elliptical spot of 48 × 22 μm (dubbed "large spot"), or smaller 2.0 ± 0.1 nA beam focussed to a spot of 25 × 17 μm (dubbed "small spot"). Smaller spot was mainly used for analyses of small crystals of minerals rich in U and Th, mainly Ca-phosphates apatite and merrillite. The dimensions and areas of the craters produced during these analyses are shown in Fig. 1a–d. During the second session (analyses of four Allende CAIs in October 2023), the samples were analysed using primary O_2^- ion beam with intensity of 10.6 ± 0.8 nA, focussed to a nearly circular 32 × 29 μm spot (Fig. 1e, f). Uniform beam intensity over the spot area was achieved by using Kohler ion optics. During both sessions, the mass resolution was set at ca. 5000, with no energy filtering to maximise sensitivity. The peak sequence includes positive ions ^{172}Yb^{16}O (mass number 188), ^{204}Pb, background at mass 204.1, ^{206}Pb, ^{207}Pb, ^{208}Pb, ^{232}Th^{16}O (mass number 248), and ^{238}U^{16}O (mass number 254). Each analysis included 10 scans, with duration of ion acquisition of 10 s on ^{172}Yb^{16}O, ^{206}Pb, ^{207}Pb, ^{208}Pb and ^{232}Th^{16}O, 20–50 s on ^{204}Pb and background, and 50 s on ^{238}U^{16}O in each scan. Each measurement was set up with 10 repeated cycles and took 32 to 40 min of one spot analysis. Ytterbium is included in the sequence on the basis of anticipation that it can serve as a proxy for U and Th for the materials with extremely low contents of the latter elements that are close to, or below, the detection limit of our procedure. Yb concentrations play only a relatively minor supporting roles in

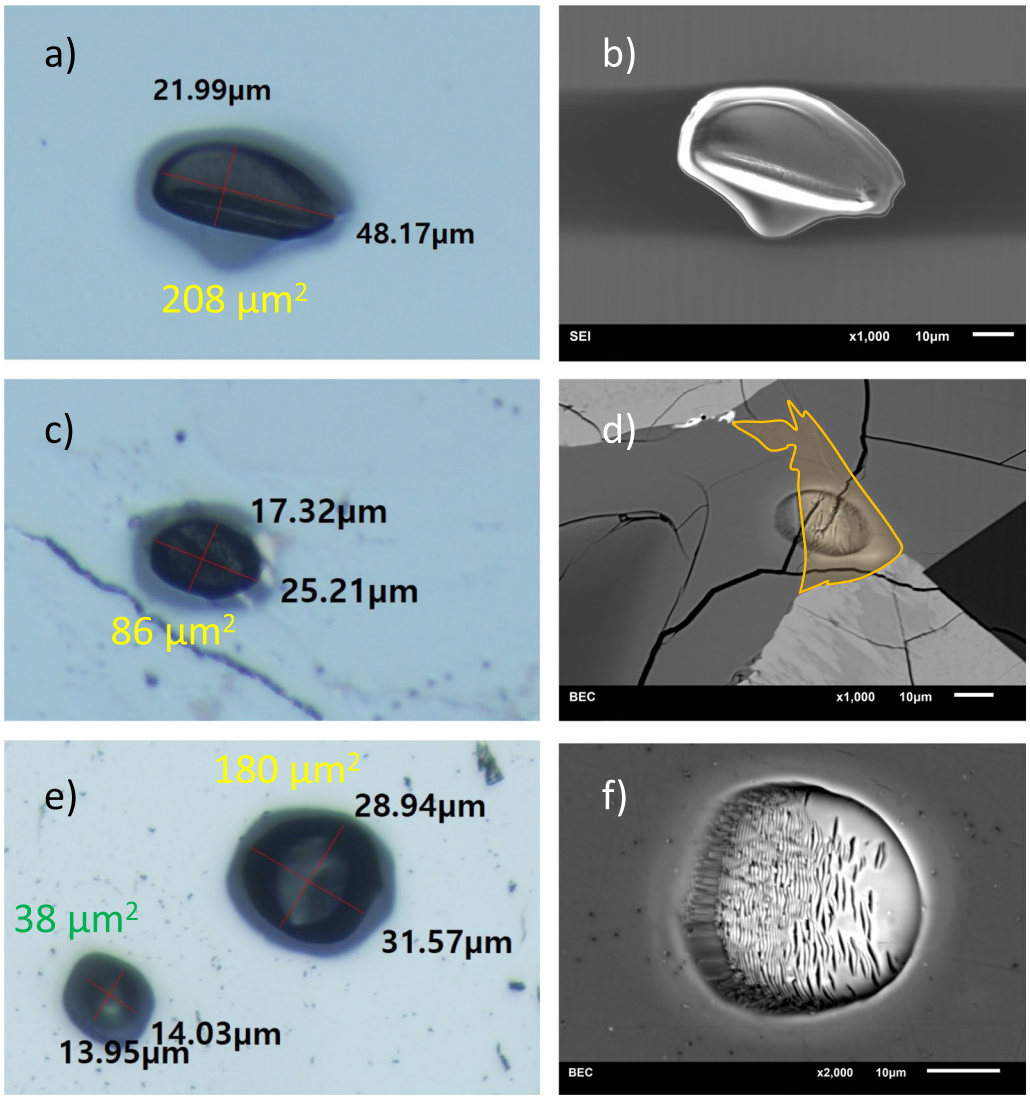

Fig. 1 Spots after SHRIMP analyses of U, Th and Pb distribution. Panes **a**, **c**, **d**—optical microscope images in reflected light, c—secondary electron image, d, f—backscattered electron images. Panes **a**,**b**—"large" spots from session 1; **c**,**d**—"small" spots from session 1, **e**,**f**—spots from session 2. The areas of spots (numbers in yellow colour) are calculated assuming elliptical shape. Orange outline shows the crystal of Ca-phosphate surrounded by silicate minerals. The SHRIMP pit is ~ 80% within the phosphate grain, and ~ 20% within silicate. The smaller 14 × 14 µm (~ 38 µm^2) spot at the bottom left corner of the pane e is a pit from oxygen isotope analysis on Cameca ims 1300 HR3 using the caesium primary beam with Gaussian profile

this study, so the discussion is focussed mainly on Th, U and Pb. Since the signal intensity during analyses of most minerals was expected to be very low, focusing of the secondary beam and peak centring were done on a material producing sufficient secondary beam intensity for all elements before the analysis of a set of 20–40 pre-programmed spots. Each spot is pre-cleaned before analysis by beam rastering for 120 s.

All measurements were taken using an ETP secondary electron multiplier (SEM). The SEM that was used during the first session was approaching the end of its usage and was operated at the voltage of 2733 V. Running the SEM at these conditions yielded the average dark noise of 0.115 ± 0.020 counts per second (cps) during the first session. The SEM was replaced shortly after the end of the first session, and the measurements of the second session were run with a new multiplier that was operated at 1966–2135 V, yielding the average dark noise of 0.015 ± 0.011 cps. The large difference in the dark noise gives us an opportunity to evaluate the influence of the background noise on the analytical performance.

The concentrations are calculated relative to the intensities of each isotope from the basaltic glass reference material (RM) BCR-2G, while NIST glasses SRM-615 and SRM-617 are analysed as secondary RMs to monitor accuracy of the concentration determinations. The element concentrations in these RMs are taken from the GeoRem database (Jochum et al. 2016), and the average value of multiple measurement of BCR-2G was used for minimising the uncertainty from the drifts of primary beam during each session. The data were primarily reduced with 'General Isotope Ratios' mode combined with 'Secondary Beam Normalization' option of the Squid v. 2.50 software (Ludwig 2009) that is used at KBSI for processing of the U, Th, and Pb data geochronological, with additional calculations performed in Excel sheets.

Results

Detection limits

Considering low concentrations of Pb, Th and U in meteorites, the detection limit (abbreviated as DL hereafter) is one of the most important parameters of the analytical procedure. The DL is a number, expressed in units of concentration, that describes the lowest concentration level of the element that can be determined to be statistically different from a blank (Long and Winefordner 1983). The exact meaning of the terms "statistically different" and "blank" depends on the nature of the analytical procedure, and in order to calculate the DL values for the measured elements using the above definition, we need to explicitly define these terms with application to concentration measurements by SIMS. The procedure described here does not involve any chemical processing of the samples before analysis, and surface contamination is eliminated by rastering, therefore the "blank" is equated with the dark noise of the SEM. The pulses in the ion counting system that constitute the dark noise, and the arrival of sample ions to the multiplier, are discrete events, and it is assumed that the dark noise and the sample signal follow Poisson statistics (e.g., Zou 2014), and the standard deviation is equal to the square root of the number of counts.

The evaluation of the minimum statistically resolved signal as a function of the total number of counts of the dark noise is shown in Fig. 2. The uncertainty of the dark noise (SD, vertical blue error bars) is square root of the total number of baseline counts during analysis. The uncertainty of the signal (vertical brown bars) is the square root of the total number of signal counts and baseline counts during sample acquisition. The minimally resolved total signal counts (brown curve) are calculated by numeric adjustment to make the lower uncertainty limits of the signal equal to the upper uncertainty limits of the background (black dashed curve). The vertical arrows corresponding to the average total baseline counts in sessions 1 (57.5 ± 7.6 counts per sample analysis) and session 2 (7.5 ± 2.7 counts per sample analysis) are projected to the intersection with the curve of minimally resolved signal counts. The minimally resolved sample signal calculated with this approach is equal to 17 counts in session 1, and 7 counts in session 2.

As an alternative to using Poisson statistics, the variability of the baseline noise can be calculated from variability of the total number of counts between the sample analyses. This approach yields the values with slightly higher uncertainties: 57.5 ± 10.0 for session 1, and 7.5 ± 5.6 for session 2. These uncertainties translate into slightly increased minimally resolved signal counts: 19 counts for session 1, and 17 counts for session 2. This approach gives a conservative estimate of the detection limit and is adopted in the rest of this study.

The calculation of the detection limits for the analysed elements is presented Table 1. The minimally resolved signal counts shown in column 7 (which are independent of the instrument sensitivity and any other analytical parameters except the background noise) are converted to the "normalised" molar DL values (column 10) by dividing by the average instrument sensitivity (counts/s/nmole/g/nA, column 9) from all analyses of the primary standard BCR-2G. The "normalised" DL values are further converted to the total molar DL values (column 11) by dividing by the integration time (number of seconds of integration of the certain isotope in one sample analysis, column 4) and by the average primary beam intensity (column 8). Finally, the total molar DL are converted to the total weight DL in parts per billion (column 12).

Analyses of NIST SRM 615 and 617 glasses

The NIST SRM 615 and 617 RMs are used as secondary standards. One or two spots from each or the primary and secondary RM were analysed before and after each sample mount. The total number of analyses of SRM 615 is 10 in the first session and 12 in the second session. The total number of analyses of SRM 617 is 11 in the first session and 8 in the second session. A complete record of individual analyses of secondary RMs is shown in the Additional file 1: Table S1.

The concentrations of Yb, Th, U and total Pb, measured in the NIST SRM 615 and SRM 617 glasses, are summarised in Figs. 3 and 4, respectively. The Yb/U and Th/U ratios are also shown. The average values with SD uncertainties are shown with yellow symbols and shaded areas. The accepted values with uncertainties (Jochum et al. 2016) are shown with red symbols and shaded areas.

The relative reproducibility (% RSD) of concentrations of Yb, Th, U and each Pb isotope, as well as total Pb, in

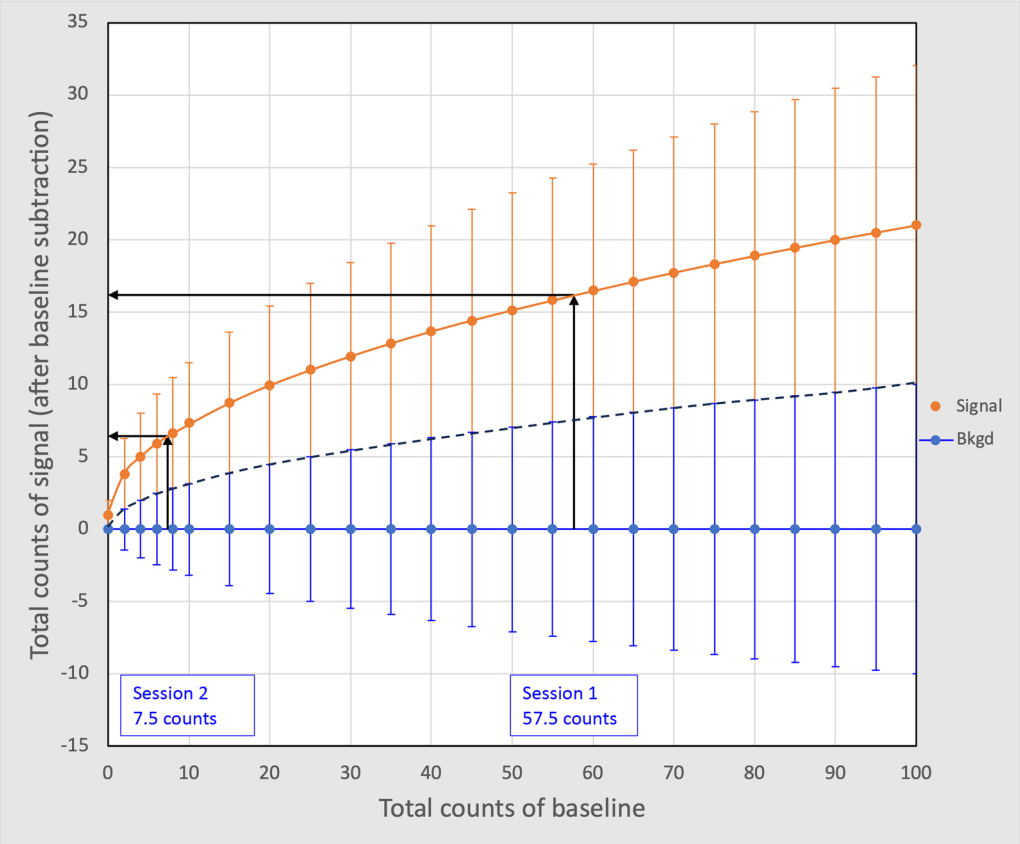

Fig. 2 Determination of the minimum resolved signal in SIMS as a function of the total number of counts of the dark noise. The uncertainty (SD) of the dark noise is calculated as a square root of the total number of baseline counts during analysis and is shown with blue vertical error bars. The uncertainty of the signal (brown vertical bars) is calculated as a quadratic sum of the signal counts and the baseline counts. The signal values (brown curve) are calculated by numeric solution to make the lower uncertainty limits of the signal equal to the upper uncertainty limits of the background (dashed curve). The average total baseline counts in sessions 1 and 2 are shown with vertical arrows and projected minimum sample counts resolved from the background—with horizontal arrows

SRM 615, is very similar between the elements, between 29 and 35%. The reproducibility of the Th/U and Yb/U ratios is much higher, at 3% and 6% RSD, respectively. The relative reproducibility of concentrations of Th, U, Pb isotopes, and total Pb in SRM 617, between 23 and 27%, is similar or slightly better than in SRM 615. The variability of the Yb concentrations is, however, about twice as large, at 65%. The reproducibility of the Th/U is slightly worse than in SRM 615, whereas the Yb/U ratios are much more variable, with RSD of 42% compared with 6% in SRM 615.

The accuracy of concentrations is good for U and Th (the certified values are within SD uncertainties of SIMS analyses for both RMs), whereas the measured Pb concentrations are about 4 times lower than the certified values. The measured Yb concentrations agree with the certified values for SRM 617, but not for the SRM 615. Likewise, the Yb/U and Th/U ratios calculated from SIMS data are consistent with the certified values for SRM 617, but not for the SRM 615.

The Yb, Th, U and Pb concentrations measured with small spots in SRM 617 significantly deviate from the data obtained with the large spots, and exclusion of the small spot data from the mean calculations substantially improves reproducibility (to 14–18% for Th, U and Pb). For SRM 615, exclusion of the small spot data produces only marginal improvement in reproducibility.

Discussion

Factors that influence the detection limits in SIMS concentration measurements

The detection limits listed in Table 1 vary from 0.2 ppb (DL for U in session 2) to ~ 30 ppb (DL for Yb in small spot analyses in the session 1). These large differences in DL depend on several factors, some of which influence the DL directly and proportionally to their change, while

Table 1 Detection limits for Yb, Th, U, and Pb

Element	At. Mass[1]	Isotope abundance	Count time, s	Noise counts	Noise uncertainty	Min. resolved sample counts	Av. primary beam, nA	Sensitivity molar[2]	DL normalised nmole/g [3]	DL total nmole/g [4]	DL total ppb [4]
1	2	3	4	5	6	7	8	9	10	11	12
Session 1, large spot (208 |jm^2)											
Yb	171.9364	0.2183	100	57.5	Poisson	17	7.5	2.56	30.41	0.0407	6.99
Yb	171.9364	0.2183	100	57.5	Measured	19	7.5	2.56	33.99	0.0454	7.81
Th	232.0381	1	100	57.5	Poisson	17	7.5	3.23	5.26	0.0070	1.63
Th	232.0381	1	100	57.5	Measured	19	7.5	3.23	5.88	0.0079	1.83
U	238.0508	0.9928	500	57.5	Poisson	17	7.5	3.41	5.03	0.0013	0.32
U	238.0508	0.9928	500	57.5	Measured	19	7.5	3.41	5.62	0.0015	0.36
206Pb	205.9745	1	100	57.5	Poisson	17	7.5	5.47	3.11	0.0042	0.86
206Pb	205.9745	1	100	57.5	Measured	19	7.5	5.47	3.48	0.0046	0.96
Session 1, small spot (86 |im^2)											
Yb	171.9364	0.2183	100	57.5	Poisson	17	2.0	2.56	30.41	0.1521	26.14
Yb	171.9364	0.2183	100	57.5	Measured	19	2.0	2.56	33.99	0.1699	29.22
Th	232.0381	1	100	57.5	Poisson	17	2.0	3.23	5.26	0.0263	6.11
Th	232.0381	1	100	57.5	Measured	19	2.0	3.23	5.88	0.0294	6.83
U	238.0508	0.9928	500	57.5	Poisson	17	2.0	3.41	5.03	0.0050	1.20
U	238.0508	0.9928	500	57.5	Measured	19	2.0	3.41	5.62	0.0056	1.34
206Pb	205.9745	1	100	57.5	Poisson	17	2.0	5.47	3.11	0.0156	3.20
206Pb	205.9745	1	100	57.5	Measured	19	2.0	5.47	3.48	0.0174	3.58
Session 2 (spot size 180 |im^2)											
Yb	171.9364	0.2183	100	7.5	Poisson	7	10.6	2.56	12.52	0.0118	2.03
Yb	171.9364	0.2183	100	7.5	Measured	17	10.6	2.56	30.41	0.0287	4.93
Th	232.0381	1	100	7.5	Poisson	7	10.6	3.23	2.17	0.0020	0.47
Th	232.0381	1	100	7.5	Measured	17	10.6	3.23	5.26	0.0050	1.15
U	238.0508	0.9928	500	7.5	Poisson	7	10.6	3.41	2.07	0.0004	0.09
U	238.0508	0.9928	500	7.5	Measured	17	10.6	3.41	5.03	0.0009	0.23
206Pb	205.9745	1	100	7.5	Poisson	7	10.6	5.47	1.28	0.0012	0.25
206Pb	205.9745	1	100	7.5	Measured	17	10.6	5.47	3.11	0.0029	0.60

[1] Atomic mass of the measured isotope

[2] Average values (counts/s/nmole/g/nA) from all analyses of the primary standard BCR-2G

[3] DL = Detection Limit. Normalised DL calculated for total integration time of 1 s and primary beam current of 1 nA

[4] Total DL is calculated with actual total integration time and average primary beam value for the session for the given spot size

Fig. 3 Concentrations of Yb, Th, U and total Pb, and Yb/U and Th/U ratios, in NIST SRM 615 glass. The Pb concentrations are sums of concentrations of individually measured Pb isotopes. Session 1 "large" spot analyses—black symbols, session 1 "small" spot analyses—blue symbols, session 2 analyses—green symbols. The average values with SD uncertainties are shown with yellow symbols and shaded areas. The accepted values with uncertainties (Jochum et al. 2016) are shown with red symbols and shaded areas

the others propagate into the DL changes in a more intricate way.

An increase of the integration time is directly propagated into decrease of the DL. The effect of the integration time is best illustrated by comparison between DL values for Th and U. Due to 5 times longer integration, the DL for U is ~ 5 times lower for any given session and spot size (the sensitivity, and the abundance of the measured isotope, are similar for both elements). Under the current conditions, the total analysis time of one spot analysis is about 40 min. Integration time for the critical peaks can be increased to improve DL, leading to the increase of the total analysis time, but longer analysis takes a greater toll of the valuable instrument time and inflicts more sample damage due to longer exposure to the primary beam.

The other major factor is the abundance of the isotope that is being measured for the concentration determination. The ca.4–5 times higher DL for Yb compared to Th, an element with similar sensitivity in SIMS and the identical integration time of 10 s per scan (100 s per analysis) is due to measuring ^{172}Yb, an isotope with ~ 22% abundance, compared with ^{232}Th with nearly 100% abundance.

The analytical sensitivity (column 9 in Table 1), the measure of the ionisation efficiency and instrument transmission, is another factor that directly affects DL. The number of counts that we get from a target under given analytical conditions is proportional to the sensitivity. In this study, we chose to measure the chemical forms of secondary ions that are produced at greater abundance by interaction of the O^- primary beam with silicate materials: oxide ions YbO^+, ThO^+ and UO^+, and

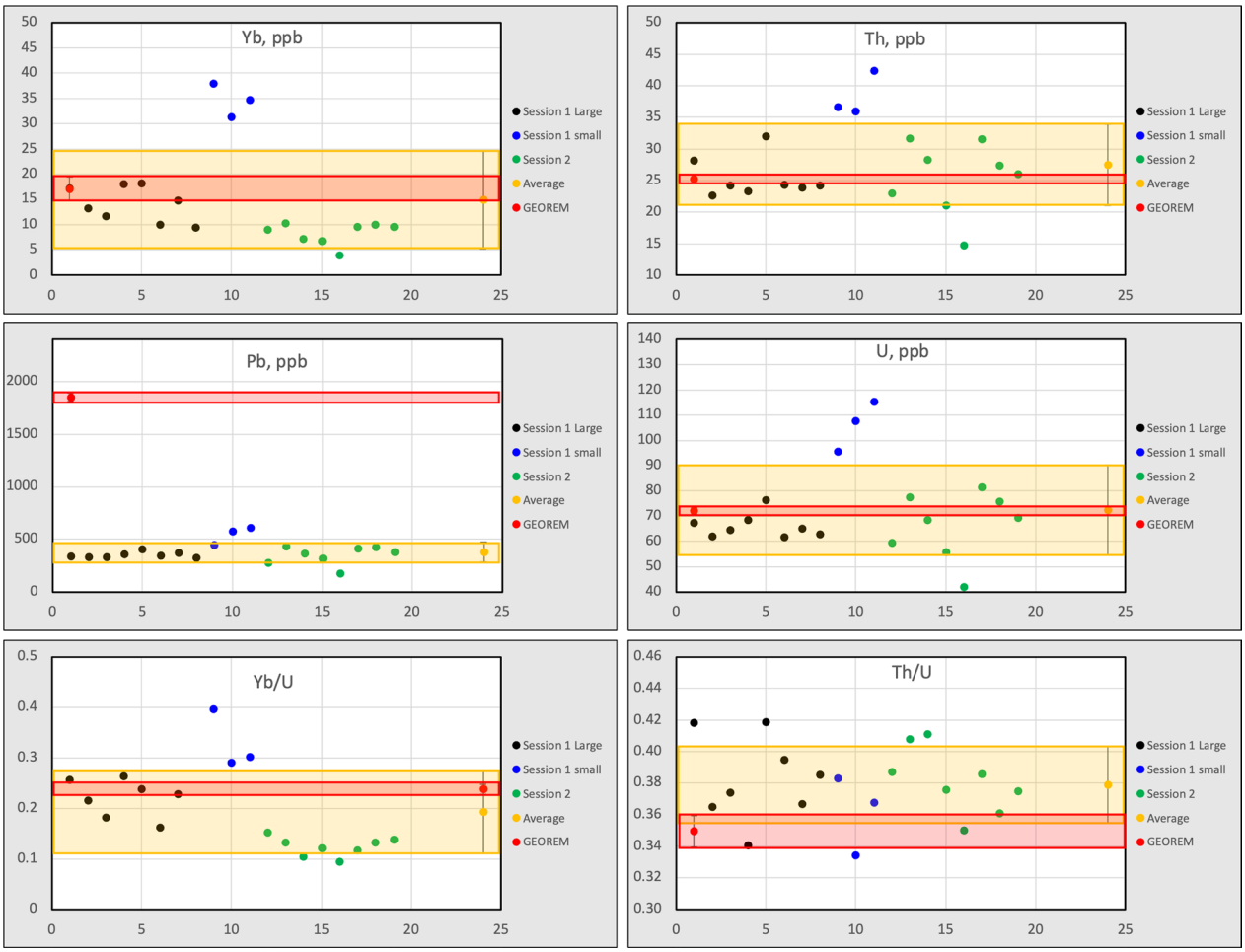

Fig. 4 Concentrations in Yb, Th, U and total Pb, and Yb/U and Th/U ratios, in NIST SRM 617 glass. The symbols and colour coding are the same as in Fig. 3

atomic ions Pb^+. Further increase of the sensitivity would require major changes in the instrument design and/or the mode of operation that would be beyond the scope of this study.

Like the analytical sensitivity, increasing the primary beam intensity directly reduces the DL values. Some of the difference in DL between the analyses in sessions 1 and 2 is due to the higher primary beam in the session 2. The primary beam intensity depends on the brightness of the primary beam source (i.e., intensity for a given area), and the aperture value (and hence the spot size). The brightness can be increased by using a modern RF plasma source instead of a duoplasmatron ion source to generate O^- ions, and using a wider aperture. However, both of these measures also reduce spatial and depth resolution, and cause more damage to the sample by more intense primary ion beam, which in turn reduces the advantage of SIMS as a nearly non-destructive method, and can compromise future additional in-situ analyses.

Reducing the baseline noise brings down the DL without any drawbacks. The effect is not linear, however. It can be quantified by the change in the minimal resolved counts between the sessions 1 and 2 shown in Fig. 2. The reduction of the average baseline noise from 57.5 to 7.5 counts (7.7 times) produced reduction of the minimal resolved counts from 17 to 7 (2.3 times) if we use Poisson statistics, but only slightly improves minimal resolved counts from 19 to 17 ppm if we use measured baseline variability. Keeping the baseline noise low and uniform is clearly advantageous and important, but it should be combined with other measures to reach the sufficiently low DL values.

The detection limit for U achieved in this study for "large" spot analyses is between 0.23 and 0.36 ppb depending on the dark noise of the used SEM and the primary beam intensity. This is ~ 30 to 50 times lower than the bulk U concentration in chondrites, and over 100 times lower than the bulk U concentrations in

eucrites, angrites and CAIs. With this DL level, we can study U distribution between all minerals, including rock-forming minerals olivine, pyroxene, plagioclase, melilite and spinel. Likewise, the detection limits of Yb, Th, and Pb are low enough to study distribution of these elements among both rock-forming and accessory minerals in chondrites and achondrites.

Precision of analyses

The reproducibility of element concentrations in secondary RMs SRM 615 and SRM 617 is mostly between ~ 20 and 30%, whereas the reproducibility of Th/U and Yb/U ratios is mostly between ~ 3 and 6%. Furthermore, the reproducibility of both elemental concentrations and the elemental ratios are similar for both RMs, despite significantly higher concentrations of three analysed elements in SRM 615 compared to SRM 617: 11 times for U, 30 times for Th, and 45 times for Yb (the Pb concentrations in both RMs are similar).

If variability of the measured concentrations was related to the factors that scale with concentration and hence with signal intensity: counting statistics, uncertainty of background subtraction, and/or isobaric interferences, we would expect substantially more variable data from the glass SRM 617 with lower concentrations of Yb, Th and U. Furthermore, we would expect similar variability of the elemental concentrations and elemental ratios. However, concentration reproducibility is similar for both secondary RMs, suggesting that variability of the measured concentrations is mainly caused by other factors: heterogeneous distribution of the elements in the primary or secondary RMs, or variability of the ion yields. Heterogeneous distribution has been documented for many trace elements in the NIST SRM 610–617 glasses (Eggins and Shelley 2002; Hu et al. 2009), and is likely to contribute to the observed variability. Variations in the SIMS ion yield (Hervig et al. 2006) are another possible contributing factor.

Variability of the sensitivity values (Fig. 5 and Additional file 2: Table S2) calculated from analyses of the primary RM BCR-2G reflects the combined effects of heterogeneity of BCR-2G and variability of ion yields. Relative contributions of these two factors cannot be directly deduced from our data, and their reliable separation would require a dedicated study. Variability of sensitivity (% RSD) for Yb, U, Th and Pb, calculated from all 25 analyses of BCR-2G during two analytical sessions (Additional file 2: Table S2) is between 22 and 25% and is similar, or only slightly smaller, than variability of concentrations of these elements in the secondary RMs (Additional file 2: Table S2). It is therefore likely that the measured variability for both primary and secondary RMs is mainly controlled by variations of the ion yield.

Two additional observations support our suggestion that variable ion yields are the principal source of dispersion of the secondary beam intensities and hence the calculated sensitivities and concentrations. Firstly, the variability of both sensitivities (Fig. 5 and Additional file 2: Table S2) and concentrations (Figs. 3 and 4, and Additional file 1: Table S1) is smaller within a single session under stable analytical conditions than calculated from the entire data set for both sessions and all beam sizes. For example, RSD of sensitivity calculated for large spot analyses in sessions 1 and 2 individually (Additional file 2: Table S2) is between 6 and 13%, compared to 22–25% for the entire data set. This difference cannot be related to the sample heterogeneity, and must reflect variations in the instrument operating conditions. Secondly, ion yield variations have effect on sensitivity for different elements making the sensitivities vary coherently over time (Fig. 5a). This greatly reduces variability of elemental ratios, which is clearly seen in both sensitivity ratios (Fig. 5b), and concentration ratios (bottom panes in Figs. 3 and 4).

We believe that the reproducibility of concentration ratios of ~ 3–6% RSD represents the uncertainty components related to the signal size (counting statistics, background noise, isobaric interferences), whereas the reproducibility of concentrations of ~ 20–30% RSD reflects mainly the variability of ion yield, and to a lesser extent, heterogeneity of the primary and secondary reference materials. The achieved concentration reproducibility is unfortunately not as good as could be expected from the sizes of the measured beams under perfectly stable instrument conditions, but it is adequate for the target application of studying U and Th distribution in meteorites. It is important that the reproducibility is not getting worse as the concentration of the measured elements in the secondary RMs are reduced. It is therefore likely that the "instrumental" component of the concentration uncertainty remains unchanged as we analyse the minerals with lower U and Th concentrations, until eventually the counting statistics becomes the dominant component of the total concentration uncertainty.

Accuracy of analyses

The data summarised in Figs. 3 and 4 show that the measured U and Th concentrations are consistent with the certified values in both secondary RMs, whereas the Pb concentrations are about 4 times lower. We have to emphasise that in this study we did not seek matrix matching between the primary RM, secondary RMs, and the unknowns, considering the range of minerals found in various types of meteorites. We also did not employ energy filtering (Shimizu 1978; Zinner and Crozaz 1986) in order to maintain the highest possible sensitivity.

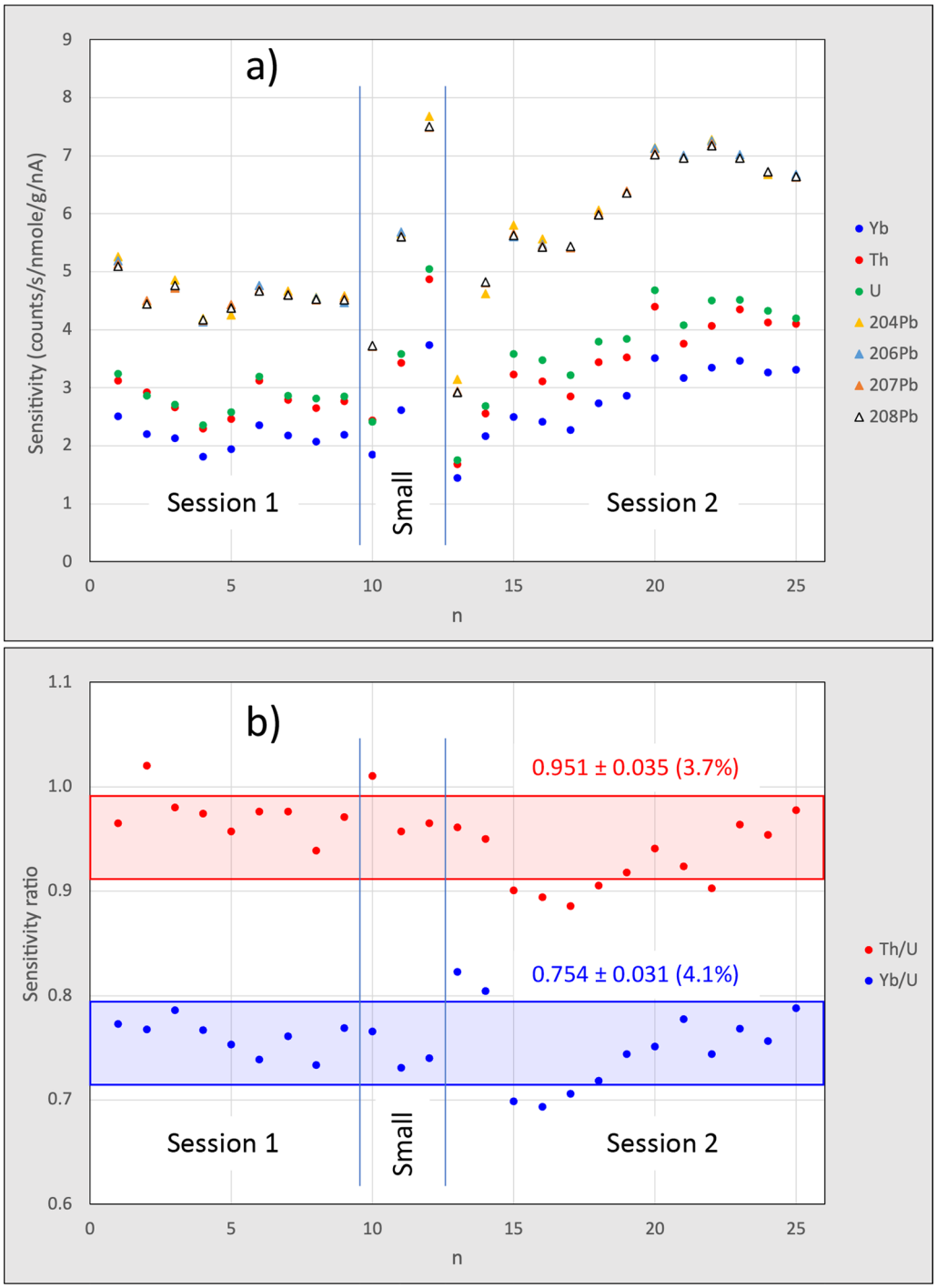

Fig. 5 Pane **a**: variations of normalised sensitivity (counts/s/nmole/g/nA) for all analysed peaks throughout the sessions 1 and 2. Pane **b**: variations of the ratios of normalised sensitivities for Th, U and Yb

The calculated concentrations bear a potential systematic uncertainty due to the dependence of ion yields on the mineral composition. Nevertheless, the concentrations of Th and U in the NIST glasses are consistent with the certified values despite the very significant compositional differences between the primary RM and secondary RMs. This consistency suggests that the concentrations of these elements measured in meteorite minerals that are compositionally closer to the primary RM are also likely to be accurate within their

random uncertainties. In contrast, the Pb concentration data should be treated as semi-quantitative until the accuracy of concentrations is confirmed by analysis of matrix-matched secondary RMs. At this point, we can only speculate why the apparent matrix effects, causing mismatched concentrations, are greater for Yb and particularly Pb, than for U and Th. This can be related to different energy distributions of atomic vs. molecular (oxide) ions, differences in volatility, differences in ionisation energies, or possibly other factors.

The isotopic compositions are not significantly affected by the matrix composition, so the measured Pb isotopic compositions can be used directly. Of course, if Pb isotopic data at higher precision are sought, for example, in U–Pb or Pb-Pb dating of U-rich meteorite minerals, then the appropriate RMs must be also analysed for Pb isotopic composition to verify instrumental mass fractionation.

The prospect of further improvements

Sensitivity, precision and accuracy of U, Th and Pb low-level concentration measurements by SIMS can be further improved from the level reported here. Some potential improvements can be achieved by relatively simple, low-tech developments, while the other would require major advancements in the instrument design.

Maintaining low detection limits requires, first and foremost, keeping the lowest possible levels of the background noise. As shown in this study, the difference in the background noise between a newly installed SEM and an SEM of the same model at the end of its lifespan accounts for more than two-fold difference in the detection limit. Using a brighter primary ion source, e.g., an RF plasma source instead of a duoplasmatron, is another measure that can boost sensitivity, although it brings a disadvantage of greater damage to the sample. Finally, simultaneous signal collection with an array of ion counting multipliers can produce a severalfold increase of effective sensitivity, with an additional benefit of less dependence of results on the primary beam stability. A multiple ion counter array was used for in-situ analysis of multiple Pb isotopes in chondrules by Bollard et al. (2017). An array of channeltron ion counters that are installed in many SIMS instruments including KBSI SHRIMP IIe may be also suitable. Channeltrons are inferior to discrete-dynode multipliers in linearity and dynamic range, and this limits their use in U–Pb geochronology and other applications with tight requirements to precision and accuracy of isotopic ratios. However, these technical limitations are likely to be irrelevant for meteorite U, Th, Pb concentration measurements, because the ion beams are consistently low, and precision of concentrations of several per cent is adequate. If the gain stability of the channeltrons is reasonable, and their dark noise is similar to the dark noise of the ETP discrete-dynode multipliers, then using an analytical setup with multiple ion counting could be advantageous.

The current precision of concentration determination is usable but certainly not ideal. Bringing the uncertainties of the concentrations down to the level of uncertainties of the elemental ratios would greatly increase the utility of the method. This would require better understanding of stability of the ion yields, and exploring the possible heterogeneity of U, Th, and Pb distribution at the scale of tens of nanometres in the primary and secondary RMs used here, to match the depth resolution of the analyses. If it is found that these elements mainly reside in nuggets or locally enriched domains, it would be necessary to look for alternative RMs with more homogeneous distribution.

Accuracy does not appear to be a problem for U and Th, at least at the current level of precision. It is, however, a problem for Pb and, to some extent, Yb. The obvious first step towards better accuracy is development of matrix-matched RMs, including their calibration with isotope dilution TIMS and MC-ICPMS, and assessment of micron-scale and nanometre-scale homogeneity. Comparative analysis of RMs by SIMS with and without energy filtering could also help to understand the nature of the observed matrix effects in concentration measurements. Using RMs that match the matrix compositions of the multitude of minerals that comprise chondrites and achondrites could significantly increase the total number of required RM analyses and hence the total duration of the analytical sessions. Using multicollection discussed above would help to mitigate that problem and keep the required analytical time within the reasonable limits.

Conclusions

We have developed a procedure for measuring low-level U, Th and Pb concentrations by peak jumping with a single discrete-dynode SEM in large ion microprobe SHRIMP IIe. The procedure is primarily intended for study of U, Th and Pb among the complete set of rock-forming and accessory minerals in meteorites, but can be also applied to other materials with concentrations of these elements in parts-per-billion range.

The limits of detection achieved in this study can be as low as 0.2 ppb for U and between 0.6 and 1.2 ppb for Pb isotopes and Th. This level of sensitivity is adequate for measuring U, Th and Pb distributions in the entire set if rock-forming and accessory minerals that constitute chondrites and achondrites, and for reconstructing of mineral inventory of these elements that is necessary for interpretation of high-precision Pb-isotopic dates. The accuracy of U and Th concentrations is confirmed by

measured concentrations of these elements in secondary reference materials NIST SRM 615 and NIST SRM 617, which match the certified values despite the huge difference in the matrix compositions of these materials and primary reference material BCR-2G. The calculated Pb concentrations, however, significantly differ from certified values. Developing a procedure that would yield accurate concentrations of all analysed elements would require closer compositional match between primary and secondary reference materials and the minerals in meteorites.

Supplementary Information

The online version contains supplementary material available at https://doi.org/10.1186/s40543-024-00439-z.

Additional file 1. **Table S1**. Raw data and processed results for secondary reference materials of NIST SRM 615 and -617.

Additional file 2. **Table S2**. Raw data and abundance sensitivity of processed results for primary reference material of USGS BCR-2G.

Acknowledgements
The authors would like to thank Ms. Shinae Lee for preparing specimens.

Author contributions
KY and YA designed this research and analysed sample with Sensitive High Resolution Ion MicroProbe. KY reduced raw data, and YA prepared the final tables and figures. YA wrote the draft of the manuscript, and KY and YA revised the manuscript.

Funding
This research was supported by Brain Pool program funded by the Ministry of Science and ICT through the National Research Foundation of Korea(grant number) (NRF-2022H1D3A2A02088853).

Availability of data and materials
All data generated or analysed during this study are included in this published article and its supplementary information files.

Declarations

Competing interests
The authors declare that they have no competing interests.

Received: 11 December 2023 Accepted: 13 April 2024
Published online: 01 May 2024

References

Amelin Y, Stern R, Krot AN. Distribution of U, Th, Pb and Nd between minerals in chondrules and CAIs. In: 34th lunar and planetary science conference, p. 1200. 2003.
Amelin Y. Meteorites (U-Pb). In: Rink WJ, Thompson JW editors Encyclopedia of Scientific dating Methods, Springer, 2015. pp. 559–562.
Bollard J, Connelly JN, Whitehouse MJ, Pringle EA, Bonal L, Jørgensen JK, Nordlund Å, Moynier F, Bizzarro M. Early formation of planetary building blocks inferred from Pb isotopic ages of chondrules. Sci Adv. 2017;3: e1700407.
Burnett DS, Stapanian MI, Jones JH. Meteorite actinide chemistry and cosmochronology. In: Barnes CA, Clayton DD, Schramm DN, editors. Essays in nuclear astrophysics. New York: Cambridge Univ. Press; 1982. p. 141–58.
Crozaz G. Uranium and thorium microdistributions in stony meteorites. Geochim Cosmochim Acta. 1979;43:127–36.
Datta C, Amelin Y, Krestianinov E, Irving AJ, Williams IS. Cooling rate paradox revealed by Pb-isotopic dating of the diabasic angrite Northwest Africa 12320. Icarus, under revision as of November 2023.
Eggins SM, Shelley JMG. Compositional heterogeneity in NIST SRM 610–617 glasses. Geostand Newsl. 2002;26:269–86.
Goreva JS, Burnett DS. Phosphate control on the thorium/uranium variations in ordinary chondrites: improving solar system abundances. Meteorit Planet Sci. 2001;36:63–74.
Hervig RL, Mazdab FK, Williams P, Guan Y, Huss GR, Leshin LA. Useful ion yields for cameca IMS 3f and 6f SIMS: limits on quantitative analysis. Chem Geol. 2006;227:83–99.
Hu Z, Liu Y, Li M, Gao S, Zhao L. Results for rarely determined elements in MPI-DING, USGS and NIST SRM glasses using laser ablation ICP-MS. Geostand Geoanal Res. 2009;33:319–35.
Jochum KP, Weis U, Schwager B, Stoll B, Wilson SA, Haug GH, Andreae MO, Enzweiler J. Reference values following ISO guidelines for frequently requested rock reference materials. Geostand Geoanal Res. 2016;40:333–50.
Jones JH, Burnett DS. The distribution of U and Pu in the St. Severin Chondrite Geochim Cosmochim Acta. 1979;43:1895–905.
Long GL, Winefordner JD. Limit of detection: a closer look at the IUPAC definition. Anal Chem. 1983;55(7):712A-724A.
Ludwig KR. SQUID 2: A User's Manual. Berkeley, Berkeley Geochron. Ctr. Spec. Pub., 2009. p 110.
Merle R, Amelin Y, Yin Q-Z, Huyskens MH, Sanborn ME, Nagashima K, Yamashita K, Ireland T, Krot A, Sieber MJ. Exploring the efficiency of stepwise dissolution in removal of stubborn non-radiogenic Pb in chondrule U-Pb dating. Geochem Cosmochim Acta. 2020;277:1–20.
Shimizu N. Analysis of the zoned plagioclase of different magmatic environments: a preliminary ion-microprobe study. Earth Planet Sci Lett. 1978;39:398–406.
Zinner EK, Crozaz G. A method for the quantitative measurement of rare earth elements in the ion microprobe. Int J Mass Spectrom Ion Processes. 1986;69:17–38.
Zou H. Error propagation. In: Treatise on Geochemistry, chapter 15.2, 2014. pp 33–42

Publisher's Note